Journal of Applied Electrochemistry **31**: 623–628, 2001.

Effect of catalyst type on the kinetics of the photoelectrochemical disinfection of water inoculated with *E. coli*

J.C. HARPER[1], P.A. CHRISTENSEN[1]*, T.A. EGERTON[1], T.P. CURTIS[2] and J. GUNLAZUARDI[3]
[1]*Department of Chemistry, Bedson Building, University of Newcastle upon Tyne, Newcastle upon Tyne, NE1 7RU, Great Britain*
[2]*Department of Civil Engineering, University of Newcastle upon Tyne*
[3]*Department of Chemistry, University of Indonesia, Kampus Baru UI-Depok 16424, Indonesia*
*(*author for correspondence)*

Received 8 June 2000; accepted in revised form 29 December 2000

Key words: disinfection, kinetics, photoelectrochemistry, sol–gel, thermal, titanium dioxide

The rates of the photoelectrochemical disinfection of *Escherichia coli* at TiO_2 electrodes were measured as a function of concentration and applied potential. Two different TiO_2 photoelectrodes were used: a thermally treated titanium plate and a porous film prepared by a sol–gel hydrolysis technique. The kinetics of the disinfection process were found to depend upon the nature of the electrode material. For the thermal film they were first order, and half order for the sol–gel film. It was also found that the catalytic activity per unit surface area of catalyst is many orders of magnitude greater than that observed using TiO_2 slurries; this was attributed to the reduced rate of electron-hole recombination afforded by the application of a small potential bias (~1 V vs Ag/AgCl), and hence the exploitation of the electric field enhancement (EFE) effect.

1. Introduction

The inactivation of pathogenic organisms is of primary importance in the treatment of domestic water supplies and is usually accomplished using chemical additives such as chlorine [1]. However, it is generally accepted that this can lead to the generation of low molecular weight chlorinated organic species in solution, some of which are harmful to humans [2], and some have been shown to provide a nutrient source for the residual bacteria in potable water. Moreover, certain pathogens including the protozoon *Cryptosporidium* are impervious to the effects of common oxidants [3, 4].

The advanced oxidation processes (AOPs) are an important class of water treatment methods which rely upon the generation of the highly oxidizing $^{\bullet}OH$ radical, which is known to kill *Cryptosporidium* [5]. The two most common AOPs involve the u.v. irradiation of either ozone or hydrogen peroxide [6]; however, the high operating costs associated with the use of such nonregenerative chemical agents have increasingly focussed the attention of chemists and engineers on the application of catalytic water treatment methods. Interestingly, $^{\bullet}OH$ radicals are also generated at the surface of TiO_2 irradiated with supra-bandgap light, and this system has already demonstrated its effectiveness in the treatment of wastewater streams [7–9].

Titanium dioxide is a wide band gap semiconductor. Irradiation with shorter wavelength light than that of the electronic band gap ($\lambda < 385$ nm anatase, 405 nm rutile) generates excess electrons in the conduction band (e^-_{cb}) and an electron vacancy or 'positive hole' in the valence band (h^+_{vb}), see Equation 1. This hole can then oxidize either surface hydroxyl ions or water to form the $^{\bullet}OH$ radical (Equations 2(a) and (b)):

$$TiO_2 + h\nu \rightarrow e^-_{cb} + h^+_{vb} \quad (1)$$

$$h^+_{vb} + H_2O_{(ads)} \rightarrow HO^{\bullet}_{(ads)} + H^+ \quad (2a)$$

$$h^+_{vb} + OH^-_{(ads)} \rightarrow HO^{\bullet}_{(ads)} \quad (2b)$$

Photocatalysis with TiO_2 to disinfect water was first reported in 1985 by Matsunaga et al. [10]. More recently, Wei et al. [11] and Belhácová et al. [12] have reported investigations into the kinetics of the disinfection of water inoculated with *E. coli* by TiO_2 slurries and an immobilized film, respectively. Wei et al. employed long wavelength u.v. lamps to mimic AM1 sunlight and reported that over 50% of the cells were killed over a period of half an hour. Belhácová et al. employed up to 7 Osram Eversun lamps above an inclined plane photoreactor utilising a film of P25 Degussa TiO_2 immobilized on a glass plate. Although other investigations have been performed on *E. coli* streams [13–16], to our knowledge the work of Wei et al. and Belhácová et al. provide the only detailed kinetic analysis.

Two major difficulties have hindered the commercial exploitation of this technology: inefficiencies due to the fast kinetics of electron hole recombination compared with the generation of hydroxyl radicals, and the separation of the small catalyst particles from the

treated effluent. This paper shows that the problems of both poor efficiency and catalyst separation can be circumvented by the use of immobilized TiO_2 electrodes. *E. coli* was selected as the target organism because it allows comparisons to be drawn between the catalytic properties of immobilized electrodes and the more widely reported TiO_2 slurry reactions.

2. Theoretical considerations

The valence energy levels of an n-type semiconductor such as TiO_2 in the absence of an electric field comprise the lowest empty (conduction) band and the topmost filled (valence) band separated by the forbidden energy gap. Just below the conduction band edge are a number of filled dopant levels, from which electrons may be thermally promoted at room temperature, giving rise to electronic conduction in the dark. The electrochemical potential of the electrons in the semiconductor is defined by the Fermi level, E_F. Irradiation of the semiconductor with supra-bandgap light results in electron–hole pairs, the majority of which simply recombine, wasting the light energy as heat.

The application of a positive potential to a TiO_2 electrode immersed in (aqueous) solution (Figure 1) decreases the energy of the Fermi level, and so results in the formation of an electric field close to the interface in a region termed the depletion layer, of thickness W. Any photogenerated electrons produced in the depletion layer will be accelerated into the bulk of the material, eventually reaching the back contact and being driven around the external circuit to the counter electrode [17]. In contrast, photogenerated holes produced within the depletion layer will be accelerated to the surface. Any holes generated within a distance $(L_p + W)$ of the surface, where L_p is the average distance over which a hole will travel before recombination in a field-free region of the semiconductor, (the minority carrier length), will diffuse to the edge of the depletion layer, and then be rapidly transported to the surface. Clearly, therefore, the electric field significantly enhances charge separation, and so increases the efficiency of $^{\bullet}OH$ radical formation, a phenomenon we have previously termed the electric field enhancement (EFE) effect [7].

3. Experimental details

3.1. *Photoelectrochemical measurements*

The photoelectrochemical reaction vessel (Figure 2) was constructed from Pyrex glass (250 ml) with two ports to allow circulation of the water. The water was pumped at a flow rate of 200 ml min^{-1}, by a peristaltic pump (Cole–Palmer 200), to afford sufficient mixing of solution. The reactor was irradiated with 2×8W UVA lamps (Philips Lighting UK Ltd, model TL/02/8, λ = 300–475 nm, λ_{max} = 360 nm) positioned 6 cm above the reactor vessel. The light intensity was measured using an Optronic Laboratories Inc. 730A radiometer and by chemical actinometry [18] and was shown to be in the order of 8×10^{-10} Ein cm^{-2} s^{-1}. All electrochemical measurements were performed using a Sycopel AEW2 potentiostat and potentials are quoted with respect to a Ag/AgCl reference electrode unless otherwise stated. A nickel gauze electrode (10 cm $\times$ 10 cm mesh, >99%, Goodfellows) was employed as the counter electrode.

The TiO_2 thermal film electrode was prepared as described in the literature [19, 20]. The 5 cm $\times$ 5 cm $\times$ 0.2 cm titanium plates (+99.6%, Goodfellows) were first cleaned with ethanol and then placed in a furnace preheated at 700 °C for 10 min in air, after which time they were allowed to cool slowly. The resulting films were shown to be largely amorphous by X-ray diffraction, but did contain some rutile crystalline regions. The TiO_2 sol–gel electrodes were prepared from the product of the acid catalysed reaction of titanium diisopropyl acetoacetonate with water [21]. Dip-coated

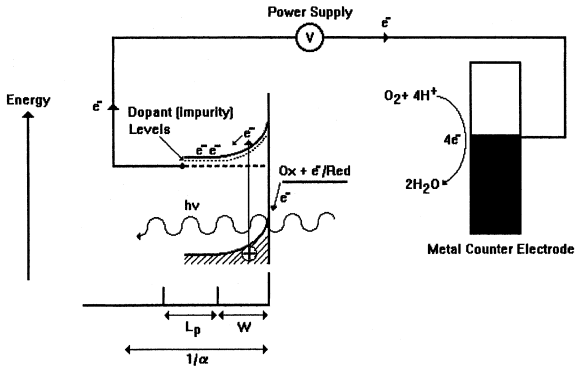

Fig. 1. Schematic representation of the events occurring during the irradiation of an n-doped semiconductor immersed in aqueous solution and under a positive potential bias with suprabandgap light. See text for details.

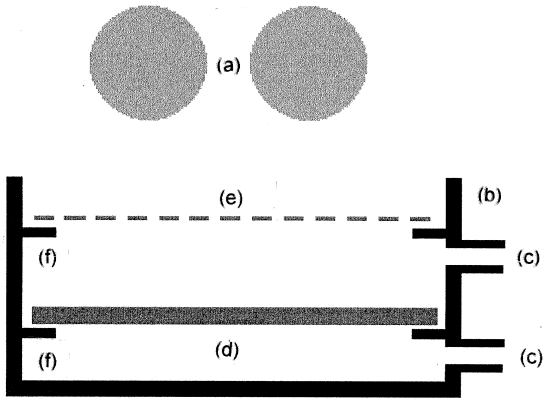

Fig. 2. Schematic representation of the photoelectrochemical reactor. (a) 2×8 W UVA lamps; (b) Pyrex glass cell; (c) inlet/outlet ports; (d) 5 cm $\times$ 5 cm $\times$ 0.2 cm TiO_2 electrode; (e) Ni mesh counter electrode; (f) glass supports. The Ag/AgCl reference electrode is omitted for clarity.

films were applied by immersing the titanium substrate into the gel product and withdrawing it slowly to ensure good coverage of the catalyst. The resulting amorphous layer was heated at 500 °C for 10 min. The procedure was repeated five times.

3.2. *Treatment of bacteriological samples*

E. coli (NCIMB, 4481) were grown overnight in a nutrient broth (Oxoid, UK). 1 cm^3 aliquots were washed once in sterile distilled water and then resuspended in 1 cm^3 of Milli-Q water. Appropriate volumes for inoculation were added to the reactor and enumerated by membrane filtration using 'membrane lauryl sulphate broth' (Oxoid, UK) as described in detail elsewhere [22].

3.3. *Effect of natural bicarbonate*

The work reported in this paper was carried out in tap water (Northumbria Water) in order to mimic as closely as possible the expected operating conditions. The analysis of the water was: Fe < 0.05, HCO_3^{2-} 22, Cu 0.09, Na 13, Mg 5.2 and K 2.9 (values expressed in mg l^{-1}).

One significant problem that has previously been encountered when employing particulate TiO_2 as a photocatalyst in natural waters is the scavenging of $^{\bullet}OH$ radicals by naturally occurring bicarbonate [3, 23, 24]. In separate cyclic voltammetry experiments using both the sol–gel and thermal film TiO_2 electrodes, the observed photocurrents at ~1.0 V did not change appreciably on the addition of 0.05 M $NaHCO_3$ to either tapwater or Millipore water containing 0.1 M $NaClO_4$, possibly as a result of the low local pH at the TiO_2 electrode surface due to the competing O_2-generation reaction.

4. Results and discussion

4.1. *Current–voltage response*

The photocurrent, which is the difference between the current observed upon irradiation with u.v. light and that observed in the dark, is a measure of the rate of charge crossing the semiconductor/electrolyte interface and thus may be taken as a measure of the rate of $OH^{\bullet}$ generation at the interface. Therefore, the photocurrents of the TiO_2 thermal and sol–gel electrodes as a function of applied potential were measured and are presented in Figures 3 and 4. The photocurrent of the thermal film is significantly greater than that of the sol–gel film. Classical semiconductor theory predicts, to a good level of approximation, that the measured photocurrent varies as [17]:

$$j_p = qI_0\left[1 - e^{-(\alpha W)/(1+\alpha L)}\right] \quad (3)$$

where j_p is the photocurrent density, q the charge on an electron, I_0 the photon flux, α the absorption coefficient,

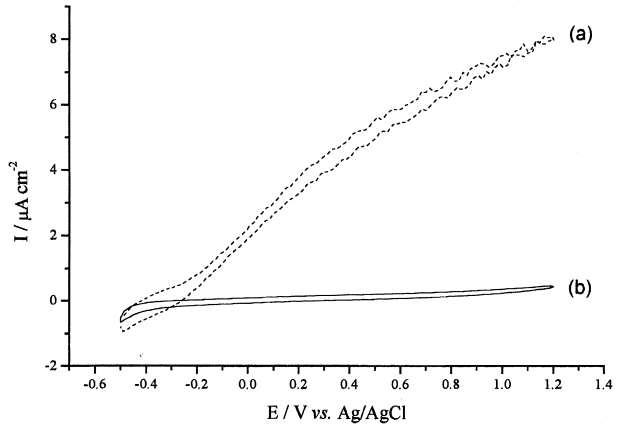

Fig. 3. Cyclic voltammograms of a thermal TiO_2 electrode in tap water (a) u.v. light on. (b) Dark response. Potential vs Ag/AgCl. Scan rate = 100 mV s^{-1}.

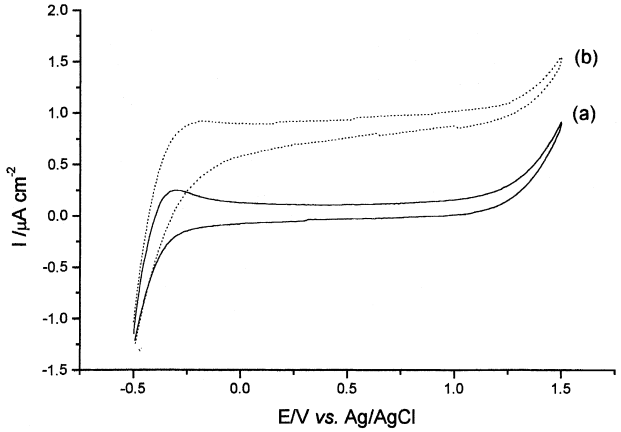

Fig. 4. Cyclic voltammograms of a sol–gel TiO_2 electrode in tap water. (a) Dark response, (b) u.v. light on. Scan rate = 100 mV s^{-1}. Potential vs Ag/AgCl.

L the minority carrier length and W is the thickness of the depletion layer. W increases with the square root of the applied overpotential according to

$$W = (2\varepsilon\varepsilon_0|V - V_f|/qN_d)^{1/2} \quad (4)$$

where ε is the relative permitivity in the direction normal to the surface, ε_0 the relative permitivity of free space, V the potential at the conduction band edge, V_f the flat band potential and N_d the donor density. For the thermal film (Figure 3), the measured photocurrent response is in general agreement with theory; Figure 5 shows a plot of the photocurrent observed during the anodic sweep of the voltammogramm in Figure 3 against $\sqrt{(V-V_{onset})}$, where V_{onset} is the potential at which anodic current is first observed in Figure 3, and V is the potential of the TiO_2 electrode. As can be seen from Figure 5, the plot is reasonably linear. However, the current–voltage response of the sol–gel TiO_2 electrode (Figure 4) does not appear to follow classical theory, as the photocurrent appears to be independent of the applied potential.

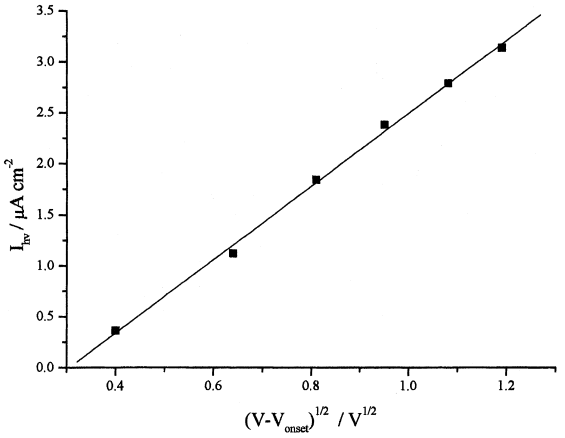

Fig. 5. Plot of photocurrent current density as a function of square root of applied potential on the thermal film TiO_2 electrode.

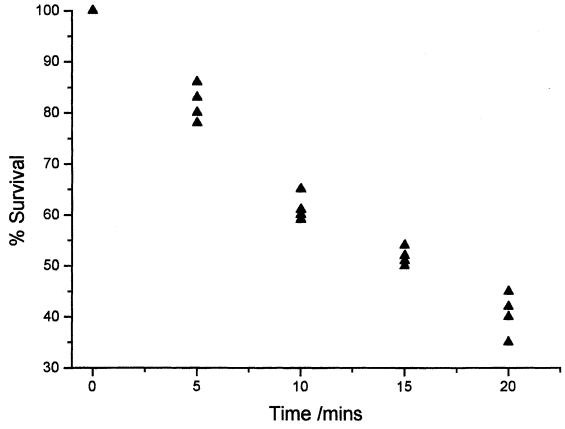

Fig. 6. A typical disinfection profile of *E. coli* (1×10^4 cells ml^{-1}) at a thermal film electrode. Potential held at 1.0 V vs Ag/AgCl (LIGHTON).

The potential-independent voltammogram in Figure 4 can be explained in terms of the work of Vinodgopal et al. [25] who reported laboratory scale studies on the photo*electro*catalytic degradation of organics in aqueous solution with the photoanode comprising undoped, particulate TiO_2 immobilized on a conducting substrate. It was stated by these authors that, in effect, the small size of the *undoped* particles would result in only a very small electric field across each particle which would be insufficient to facilitate charge separation. The fact that an increase in degradation was observed on the application of a potential to the TiO_2 electrodes was discussed in terms of an increase in the efficiency of charge separation as a result of the combination of the differing rates of electron and hole transfer at the solution interface, and the potential gradient across the whole film. Hence, the increased recombination associated with small particles can produce photocurrents which are independent of applied potential and therefore differ markedly from those predicted by Equation 3.

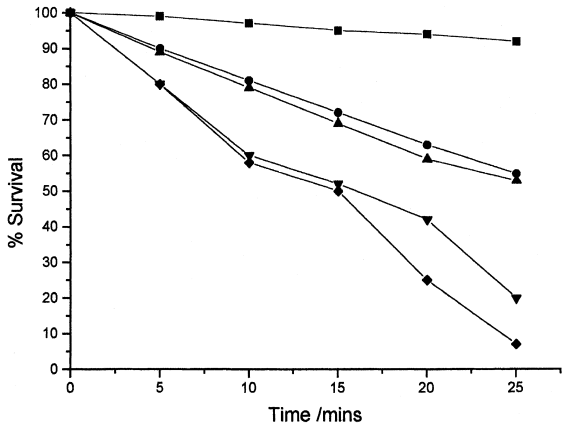

Fig. 7. Effect of applied potential on rate of disinfection of *E. coli* bacteria (1×10^4 cells ml^{-1}) at a TiO_2 thermal film. Potentials vs Ag/AgCl. Experimental conditions: (■) light off at open circuit, (+) light off at 1.0 V, (●) light on at 0.1 V, (▲) light on at open circuit, (▼) light on at 0.5 V and (◆) light on at 1.0 V.

4.2. *Effect of potential on the rate of disinfection*

The results from a typical disinfection experiment are presented in Figure 6. They demonstrate the statistical spread of results associated with counting replicate cultures developed from the same sample. To obtain representative correlations the disinfection rate was taken as the geometric mean of four readings. The effect of the applied potential on the rate of disinfection at a thermal film is presented in Figure 7. An increase in rate of reaction is observed with increasing bias potential, in agreement with the data in Figure 3. Figure 8 shows the disinfection of the same concentration of cells at a sol–gel electrode and the rate of reaction appears to be potential-independent, which is also fully consistent with data in Figure 5. The practical implications of these results are that TiO_2 thermal electrodes should be operated at high anodic (V = 1.0 V vs Ag/AgCl) potentials while potentials as small as −0.25 V, that is,

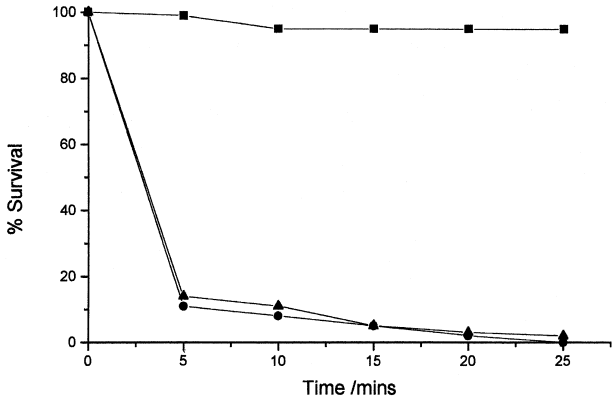

Fig. 8. Effect of applied potential on rate of disinfection of *E. coli* bacteria in tap water (1×10^3 cells ml^{-1}) at a TiO_2 sol–gel electrode. Potentials vs Ag/AgCl. Experimental conditions: (■) light off at 1.0 V, (▲) light on at 0.5 V and (●) light on at 1.0 V.

close to the plateau region in Figure 4, are sufficient to drive the reaction at sol–gel TiO_2 electrodes.

4.3. *Kinetics of the disinfection process*

The effect of the initial cell concentration upon the rate of disinfection at a TiO_2 thermal film is presented in Figure 9, from which it is apparent that the kinetics of the reaction are strongly influenced by the initial density of *E. coli* in the reservoir. A plot of log r_i against log c_i (where r_i is the rate of disinfection, cells min^{-1} cm^{-3}, and c_i is the concentration of cells per cm^3), at four different *E. coli* concentrations using the thermal film electrode is shown in Figure 10, along with an analogous plot for the sol–gel electrode. From the plot the reaction order for the thermal film data was calculated to be 0.93; in other words approximately first order,

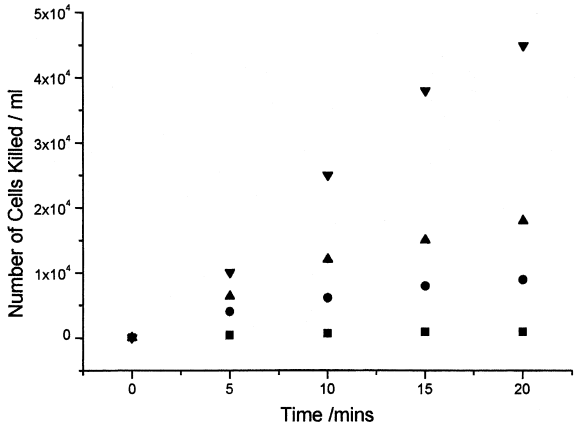

Fig. 9. Number of cells killed per millilitre of sample against time at a TiO_2 thermal film. Initial cell concentrations expressed as cells ml^{-1}: (■) 1×10^3, (●) 1×10^4, (▲) 3×10^4 and (▼) 1×10^5.

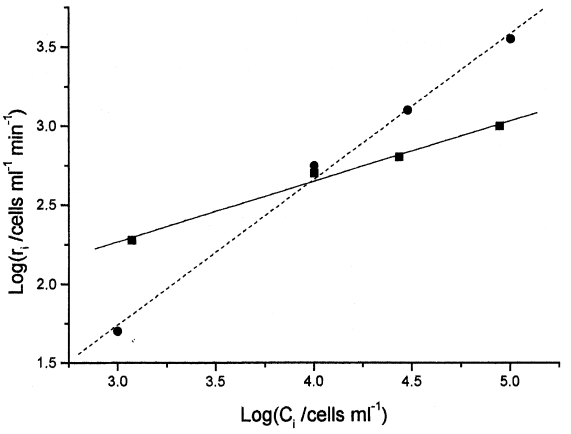

Fig. 10. Plot of log initial rate of reaction at sol–gel (——) and thermal film (- - - -) electrodes against log initial concentrations of *E. coli* in the range 1×10^3 to 1×10^5 cells ml^{-1}. Electrolysis performed under potentiostatic control (1.0 V vs Ag/AgCl).

which is consistent with the work of Wei and coworkers at similar concentrations, but using a TiO_2 slurry [11].

Belhácová et al. [12] also found that the rate of decrease in *E. coli* cell viability was directly proportional to the initial cell concentration, in agreement with first order kinetics. In both cases, the light intensities employed were generally higher than in our own experiments, (8×10^{-10} Ein cm^{-2} s^{-1}); thus the light intensities employed by Wei et al. were from 180×10^{-10} Ein cm^{-2} s^{-1} to 1660×10^{-10} Ein cm^{-2} s^{-1}, while Belhácová et al. employed intensities between about 9×10^{-10} Ein cm^{-2} s^{-1} and 62×10^{-10} Ein cm^{-2} s^{-1}. The first order rate constant for the thermal film in Figure 7 was calculated to be $k = 1.16 \times 10^{-1}$ min^{-1} compared to about 1.3×10^{-1} min^{-1} to 8.3×10^{-1} min^{-1}, (depending upon the light intensity), observed by Wei et al., and about 0.7×10^{-1} min^{-1} to 1.4×10^{-1} min^{-1} observed by Belhácová et al. At the same concentration of *E. coli*, the rate constant observed by us was about twice that reported by Wei et al. In addition, if the rate of disinfection per unit surface area is calculated and the results compared with those of Wei et al., the application of an electric field enhances the rate of disinfection by a factor of approximately 1×10^5 (Degussa P25 has a surface area of 50 m^2 g^{-1} [26], thermal film electrode ~25 cm^2).

It is interesting to note that, on increasing the light intensity by a factor of ~3, Belhácová et al. observed a concommittant increase in disinfection rate of only ~2, which is suggestive of the $\sqrt{}$(Intensity) dependence of the photoactivity of TiO_2 previously noted in detoxification [3] and paint durability [27] studies. However, Wei et al. observed a linear increase in the rate constant with increasing light intensity.

Analysis of the results at the sol–gel film strongly suggests that a more complex rate law applies. The slope of the plot of log r_i against log c_i yielded a value of 0.43, suggesting a half order reaction and the half order rate constant was calculated to be 8 $cells^{1/2}$ $ml^{-1/2}$ min^{-1}. The fact that different kinetics were observed at the two types of electrode strongly suggests that the surface process is rate limiting, a postulate supported by the fact that turning off the peristaltic pump had no effect upon the observed kinetics.

The postulate that the kinetics of the photoelectrochemical destruction of *E. coli* depend upon the type of TiO_2 electrode is in very interesting, and is in agreement with our previous work in which the rate of disinfection of *Cryptosporidium parvum* spores was found to be dependent upon the nature of the electrode material employed [28]. This is currently under further investigation.

The practical implications of these findings are potentially significant for the design of effective pilot plant reactors. The results suggest that a two-component disinfection reactor should be employed, wherein initial high cell concentrations are reduced using a thermal film-based system, after which the final 'polishing' process is carried out using sol–gel electrodes.

4.4. *Quantum yield*

A significant cost component of any commercial photo-electrochemical disinfection process would be the cost of the u.v. source, and hence an important aspect of the technology is the quantum yield. In the present study, the (charge carrier) quantum yield for the process is defined as

$$\Phi = \frac{\text{number of electrons in the external circuit}}{\text{number of incident photons}} \times 100 \quad (5)$$

The values determined on this basis were 1.7% and 0.6% for the thermal and sol–gel films at 1.0 V, respectively. These values correspond to a production of hydroxyl radicals of the order of $2 \times 10^{14}\ s^{-1}$, assuming that the number of electrons crossing the interface (i.e., the photocurrent) equals the number of hydroxyl radicals produced per second. However, the rate of disinfection is in the order of approximately 30 cells $s^{-1}\ cm^{-3}$ which suggests that many $^{\bullet}OH$ radicals are consumed by alternative reaction pathways, such as dimerization to give, eventually, molecular oxygen [29, 30], and hence are essentially ineffective.

Since the choice of lamp can alter the kinetics of a degradation process, it is somewhat unfortunate that there is no standard light source to which all other data is compared and consequently comparisons between studies are always empirical. For example, the rate of electron-hole generation is extremely sensitive to the wavelength and intensity of the incident radiation [31]. It is the aim of a future publication to illustrate the effects of the lamp in terms of light intensity and spectral distribution upon the kinetics of disinfection.

5. Conclusions

This study confirms previous work which has shown that the application of a small potential bias can significantly increase the rate of disinfection of *E. coli* suspensions at u.v.-irradiated TiO_2 electrodes. These electrodes provide a potentially robust and cheap source of $^{\bullet}OH$ radicals for water treatment without the need for high power, short wavelength u.v. lamps. It is clear from this work that the nature of the TiO_2 electrodes affects not only the rate of disinfection, but also the order of the reaction; consequently, electrodes prepared via the thermal oxidation of titanium metal at 700 °C are more effective at high *E. coli* concentrations, whereas electrodes produced via a sol–gel process are more effective at low concentrations. The electrochemical characterization of the different electrodes suggests that the observed differences may be due to the smaller particle size of the sol–gel derived films and consequent decrease in the 'electric field enhancement' effect.

Further work to characterize the TiO_2 electrodes and hence increase their photo-electrochemical efficiency is in progress.

Acknowledgements

The authors would like to acknowledge the financial support of the EPSRC (grants GR/L 13360 and GR/L 96066).

References

1. T. Matsunaga and M. Okochi, *Environ. Sci. Technol.* **29** (1995) 501.
2. L.A. Lawton and P.K.J. Robertson, *Chem. Soc. Rev.* **28** (1999) 217.
3. P.A. Christensen and G.M. Walker, *'Opportunities for the UK in Solar Detoxification'*, ETSU s/P4/00249/REP (1996).
4. A.T. Campbell, L.J. Robertson, M.R. Snowball and H.V. Smith, *Wat. Res.* **29** (1995) 2583.
5. N.A. Simmons, *Biologist* **38** (1998) 147.
6. J.C. Ireland, 'Photocatalytic Purification and Treatment of Water and Air' (Elsevier, 1993) pp. 557–571.
7. I.M. Butterfield, P.A. Christensen, A. Hamnett, K.E. Shaw, G.M. Walker, S.A. Walker and C.R. Howarth, *J. Appl. Electrochem.* **27** (1997) 385.
8. S.A. Walker, P.A. Christensen, K.E. Shaw and G.M. Walker, *J. Electroanal. Chem.* **393** (1995) 137.
9. M.R. Hoffmann, S.T. Martin, W. Choi and D.W. Bahnemann, *Chem. Rev.* **95** (1995) 69.
10. T. Matsunaga, T. Nakajima, R. Tomada and H. Wake, FEMS *Microbiol. Lett.* **29** (1985) 211.
11. C. Wei, W.Y. Lin, Z. Zulkarnain, N.E. Williams, K. Zhu, A.P. Kruzic, R.L. Smith and K. Rajeshwar, *Environ. Sci. Technol.* **28** (1994) 934.
12. L. Belhacova, J. Krysa, J. Geryk and J. Jirkovsky, *J. Chem. Technol. Biotechnol.* **74** (1999) 149.
13. T. Matsunaga, R. Tomoda, T. Nakajima, N. Nakamura and T. Komine, *Appl. Environ. Microbiol.* **54** (1988) 1330.
14. T. Matsunaga, R. Tomoda, T. Nakajima and H. Wake, *Microbiol. Lett.* **29** (1985) 211.
15. P. Zhang, R.J. Scrudato and G. Germano, *Chemosphere*, **28** (1994) 607.
16. J.C. Ireland, P. Klostermann, E.W. Rice and R.M. Clark, *Appl. Environ, Microbiol.* **59** (1993) 1668.
17. A. Hamnett, *Comprehensive Chemical Kinetics* **27** (1987) 61.
18. J.G. Calvert and J.N. Pitts, 'Photochemistry', (*J. Wiley & Sons,* New York, 1966) pp. 782–785.
19. Y. Choi, S. Seo, K. Chjo, Q. Choi and S. Park, *J. Electrochem. Soc.* **139** (1992) 1803.
20. T. Yoko, A. Yuasa, K. Kamiya and S. Sato, *J. Electrochem. Soc.* **138** (1991) 2279.
21. L. Kavan and M. Gratzel, *Electrochim. Acta* **40** (1995) 643.
22. The Standing Committee of Analysts, 'The Microbiology of Water 1994, Part 1-Drinking Water' (HMSO, London, 1994).
23. O. Legrini, E. Oliveros and A.M. Braun, *Chem. Rev.* **93** (1993) 671.
24. K. Rajeshwar, *J. Appl. Electrochem.* **25** (1995) 1067.
25. K. Vinodgopal, U. Stafford, K.A. Gray, P.V. Kamat, *J. Phys. Chem.* **98** (1994) 6797.
26. A.M. Mills and S. Le Hunte, *J. Photochem. Photobiol.* **108** (1997) 1.
27. P.A. Christensen, A. Dilks, T.A. Egerton and J. Temperley, *J. Mater. Sci.* **35** (2000) 5353.
28. P.A. Christensen, T.P. Curtis, B. Place and G.M. Walker, *Water Res.*, submitted.
29. M.L. Garcia Gonzalez and P. Salvador, *J. Phys. Chem.* **88** (1984) 3696.
30. M.L. Garcia Gonzalez and P. Salvador, *J. Electroanal. Chem.* **325** (1992) 369.
31. C.J. King and T.A. Egerton, *J. Oil Col. Chem. Assoc.* **62** (1979) 386.